urban science

MDPI

Article

Parametric Optimization of Urban Street Tree Placement: Computational Workflow for Dynamic Shade Provision in Hot Climates

Samah Elkhateeb [1,2] and Raneem Anwar [2,*]

[1] Architectural Engineering, University of Business and Technology (UBT), Jeddah 21448, Saudi Arabia; samah.elkhateeb@eng.asu.edu.eg
[2] Smart and Future Cities Laboratory for Sustainable Urban Solutions, Faculty of Engineering, Ain Sham University, Cairo 11517, Egypt
* Correspondence: raneem_abdulghany@hotmail.com

Abstract

Urban streets in hot climates often suffer from inadequate shade, exacerbating pedestrian discomfort, urban heat island effects, and energy demands for cooling. Traditional tree-planting approaches overlook dynamic solar paths, building-induced shadows, and spacing requirements, resulting in suboptimal shade coverage and resource inefficiency. This study introduces a computational workflow in Rhino/Grasshopper to optimize tree placement and canopy radii through analysis of solar radiation and shadow patterns. By prioritizing sun-exposed zones, minimizing shadow overlaps, and ensuring growth-appropriate distances, the tool enhances shade distribution. Integration of parametric modeling and environmental simulations improved thermal comfort, reduced energy use, and evidence-based urban planning strategies. Across ten optimization runs, the workflow achieved a 68% increase in shade coverage, an 11.5 °C reduction in mean radiant temperature (MRT), and a 72% decrease in the spatial extent of high-risk heat-exposure zones, demonstrating its potential for climate-adaptive street design in hot-arid environments.

Keywords: parametric optimization; urban tree placement; shade provision; hot climates; computational workflow; climate-responsive parametric design

check for updates

Received: 15 October 2025
Revised: 25 November 2025
Accepted: 26 November 2025
Published: 28 November 2025

Citation: Elkhateeb, S.; Anwar, R. Parametric Optimization of Urban Street Tree Placement: Computational Workflow for Dynamic Shade Provision in Hot Climates. *Urban Sci.* **2025**, *9*, 504. https://doi.org/10.3390/urbansci9120504

Copyright: © 2025 by the authors. Licensee MDPI, Basel, Switzerland. This article is an open access article distributed under the terms and conditions of the Creative Commons Attribution (CC BY) license (https://creativecommons.org/licenses/by/4.0/).

1. Introduction

In hot climates, inadequate street-level shade increases building cooling requirements, increases urban heat islands, and worsens pedestrian heat stress. Increased energy use for air conditioning and health risks like heat fatigue can result from high solar exposure during peak hours, which can raise surface temperatures by 10 to 20 degrees Celsius above shaded locations [1]. In dense urban environments, where the predominance of impermeable surfaces exacerbates heat retention and diminishes thermal resilience, shade, evapotranspiration, and vegetation structure are significant factors of microclimatic comfort, according to fundamental urban design research [2]. Through canopy shading, albedo modulation, and localized cooling, green infrastructure, especially trees—plays a demonstrated role in reducing these impacts; nevertheless, its implementation is still uneven and frequently non-strategic [3].

Existing tree-planting initiatives, while beneficial for biodiversity and aesthetics, frequently rely on uniform grids or aesthetic preferences rather than data-informed strategies [4]. Recent advances in urban tree placement optimization have resulted in the devel-

opment of GIS-based solar access models capable of mapping irradiance at the city scale and more precisely identifying high-exposure hotspots [5]. Concurrent advances in agent-based pedestrian behavior simulations (ABM) have enabled the modeling of micro-scale pedestrian flows, thermally comfortable route selection, and visibility-based navigation. However, the practical application of these two domains—GIS solar modeling and ABM movement simulations—for shade-specific, street-level tree placement is limited [5,6].

Studies on urban forestry highlight that ignoring variables such as seasonal solar angles, pedestrian exposure duration, building heights, and dynamic shadow trajectories leads to shading being inefficiently distributed and cooling already shaded areas while leaving true hotspots untreated [7–10]. Moreover, inadequate spacing can also reduce long-term canopy performance, increase maintenance costs, and damage tree health. While ABM captures emergent pedestrian behavior and GIS excels at large-scale radiation mapping, neither framework can support parametric, street-scale optimization that considers solar geometry, canopy morphology, spatial constraints, and biological requirements such as root-zone spacing [11,12].

Hence, environmental design research has used technologies such as GIS for large-scale planning, but these are insufficient for micro-spatial optimization, especially when solar exposure and parametric adjustability are needed [13]. This results in significant methodological disparity. The lack of an integrated, computational pipeline capable of optimizing tree placement based on solar exposure and pedestrian use patterns at the street scale [12,14].

In order to bridge this gap, the current study presents PATHSHADE, a computational methodology that combines evolutionary optimization, solar-radiation simulation, and parametric modeling and is implemented in Rhino/Grasshopper. By integrating Galapagos-driven tree-position optimization into a street-level, pedestrian-focused framework, PATHSHADE expands GIS solar access modeling. The main innovation of this study is the combination of astronomical ephemeris calculations for solar geometry, behavior-informed pathway prioritization, and biologically constrained canopy modeling, which addresses the drawbacks of set planting layouts and static shading assessments.

This method simulates dynamic radiation patterns and building shadows by importing site geometry and astronomical ephemeris calculations for solar data. Priority shade zones are determined by applying algorithmic procedures to assess pedestrian walkways that are exposed to the sun. While enforcing restrictions like minimum spacing, root-zone protection, and avoiding redundant shadow overlaps, optimization algorithms modify tree placement and canopy radii to maximize shade. Rapid prototypes customized to site-specific conditions are produced by subsequent environmental simulations that quantify shaded area percentages and thermal load reductions. This project offers a fully parametric, solar-responsive, and reproducible methodology for optimizing tree planting in urban streetscapes in hot climates, in contrast to earlier approaches.

Therefore, the primary objective of this research is to create an integrated computational workflow that maximizes shade performance in hot climates by optimizing urban tree planting. To guide this objective, the following questions are posed:

Q1. *How can dynamic solar radiation, pedestrian movement patterns, and biological spacing constraints be integrated into a single parametric optimization framework for street-level tree placement?*

Q2. *To what extent can an evolutionary optimization approach improve shade coverage and reduce mean radiant temperature (MRT) compared to conventional or static planting strategies?*

Q3. *How can computational results be translated into actionable design guidelines that support planners in implementing climate-responsive tree-placement strategies in data-limited contexts?*

2. Why Traditional Urban Design Fails to Address Extreme Heat

Traditional urban planning, rooted in historical practices of organizing urban spaces, often falls short in addressing the escalating challenge of extreme heat, particularly in the context of climate change and the urban heat island (UHI) effect [15,16]. This failure stems from systemic limitations that hinder the ability to create thermally comfortable, resilient urban environments, setting the stage for the need to explore more integrated, adaptive approaches [17].

The first major restriction is a lack of cross-disciplinary collaboration and segregated governance mechanisms. Historically, land use, infrastructure, and environmental management choices have been determined independently within strong departmental boundaries in urban planning. [18]. Understanding the intricate dynamics of urban heat requires the important input of climatologists, environmental scientists, and public health specialists, all of whom are not included in this disjointed approach [19]. Planners wouldn't have the broad perspective needed to address excessive heat as a complicated issue that affects public health, energy use, and infrastructure resilience without this kind of collaboration. Furthermore, due to a lack of information on local microclimates and patterns of heat exposure, personalized measures are often constrained by the inadequacies of traditional planning [20]. For instance, if planners lack complete data on temperature differences between neighborhoods, they are unable to allocate resources for the most susceptible communities, which leads to them obtaining insufficient protection against rising temperatures.

This lack of integration creates a discrepancy between policy objectives and the actual risks of heat exposure, weakening the effectiveness of municipal efforts. Because traditional urban planning is unable to synchronize various plans, such as housing, transportation, and environmental policies, there is sometimes a disconnect between policy goals and urban residents' actual experiences [21]. Policies may prioritize economic development or infrastructure expansion without considering how these decisions affect heat absorption by increasing the use of impermeable surfaces such as concrete and asphalt. As a result, communities that are most vulnerable to excessive heat—typically those with low incomes or dense populations—receive less funding and attention. Because of this mismatch, vulnerable communities are disproportionately affected by rising temperatures, making it difficult to create equitable heat resilience and potentially leading to health problems, decreased productivity, and financial pressure [22].

The dependence on ineffective tools like density regulations and zoning, which are ill-suited to manage thermal comfort or lessen the UHI effect, exacerbates these problems. Economic efficiency or aesthetic consistency is frequently given precedence over environmental considerations in zoning restrictions, which are intended to separate land uses and control urban sprawl [21,23]. These technologies do not include the thermal properties of roadway layout, vegetation cover, or urban materials, all of which have a significant impact on urban heat. For example, zoning that disregards opportunities for green spaces that could provide shade and evaporative cooling may permit huge concrete developments that absorb and retain solar radiation, so increasing the UHI effect [15]. In a similar vein, density limits may inadvertently encourage high-rise building with meandering street canyons that trap heat and impede airflow, elevating urban temperatures. These methods disregard approaches of dealing with excessive heat, such as reflective building materials or passive cooling measures, which are critical for developing sustainable urban environments in the face of rising global temperatures [24].

Furthermore, conventional urban planning frequently ignores the significant effects of climate change and the UHI effect, neglecting to incorporate adaptive methods that might protect urban infrastructure, public health, and economic stability. Heatwaves brought on by climate change intensify the UHI effect, which occurs when urban areas have greater

temperatures than their rural surrounds because of heat-retaining materials and human activity [25]. However, traditional planning has always ignored outdoor spaces where residents spend a lot of time in favor of indoor comfort through mechanical cooling systems.

Given that extended exposure to intense heat can result in heatstroke, respiratory problems, and cardiovascular strain, this oversight jeopardizes public health [26]. Economically, increased demand for cooling raises energy costs, stresses urban infrastructure, and increases greenhouse gas emissions, all of which exacerbate climate change [17]. Because traditional urban planning ignores these cascading impacts, cities are unprepared to deal with the growing frequency and intensity of heat waves. Finally, typical urban planning relies on one-size-fits-all solutions that neglect site-specific variances, microclimate complexity, and the necessity for customized UHI mitigation techniques. Microclimates in urban areas vary depending on building height, street direction, and land cover [27].

Conventional methods often ignore regional heat exposure in favor of applying homogeneous treatments throughout entire cities. Strategies such as land-use planning that prioritize green infrastructure, such parks and urban woods, which can lower temperatures through evapotranspiration and shading, are necessary for effective UHI mitigation [28]. Although they are sometimes overlooked in conventional planning, passive cooling strategies are as important. Examples include the use of high-albedo materials for pavements and rooftops or the design of street layouts to improve ventilation [16]. This lack of adaptive methods makes urban people more susceptible to thermal stress and reduces the general livability of cities as climate change increases the frequency of high heat events. When taken as a whole, these flaws highlight the pressing need for a paradigm change toward climate-responsive urban design, which immediately fills in the gaps by placing an emphasis on integration, data-driven decision-making, and adaptable tactics.

3. The Emergence of Climate-Responsive Urban Design

Climate-responsive urban design (CRUD) has emerged as a critical discipline in response to the intensifying impacts of global warming on urban livability, particularly in addressing extreme heat and the UHI effect [9]. This strategy starts with the understanding that urban communities must adapt to climate change while maintaining a common urban identity [27], employing substantial body of information to guide resilience and sustainable development. However, there are particular difficulties when implementing CRUD in high-density informal urban neighborhoods in hot, dry climates, such as severe weather that is exacerbated by a lack of financial resources and regulatory frameworks [29].

At its core, CRUD mediates the interplay between site, climate, and human needs by strategically combining spatial elements to shield urban spaces from adverse climatic effects while enhancing beneficial ones [30,31]. However, a gap remains between CRUD's theoretical focus on multifunctional green infrastructure (GI) and its street-scale computational implementation, where site-specific factors such as solar geometry, pedestrian flows, and biological constraints (such as 4–8 m root buffers) necessitate parametric precision beyond static guidelines [8].

This extensive topic considers seasonal variations in the microclimate, with a focus on lowering midsummer urban heat accumulation due to its considerable impacts on infrastructure, health, and mortality [29]. Thermal comfort, defined by prevailing environmental conditions such as temperature, humidity, and solar radiation, has a substantial impact on the decision to use and stay in outdoor urban spaces [16]. CRUD addresses these problems by utilizing adaptation methods such as urban canopies for localized cooling and mitigation strategies such as green roofs and urban parks to lower citywide air temperatures [30]. These solutions improve the year-round usability of public spaces by increasing heat escape from urban surfaces and encouraging evaporative cooling via plant and water features.

A key feature of CRUD is the creation of "urban cool spots," such as squares, shaded seating areas, and street furniture, designed to lower perceived temperatures and serve as comfortable gathering spots during hot periods [28]. These spaces integrate temporary measures, like misting canopies, and permanent features, such as water elements, to modify microclimatic factors on a human scale. Although parametric precedents, like generative design in Revit-Dynamo for Egyptian communal spaces, have optimized tree distributions to achieve 52–68% shade coverage and 9–11.5 °C MRT reductions, they also highlight implementation challenges, such as an excessive dependence on uniform grids that worsen canopy collisions in constrained morphologies [32,33]. These spaces naturally evolve into social gathering venues by enhancing thermal comfort and integrating community engagement with climate-responsive design. CRUD emphasizes the utilization of vegetation to mitigate urban environmental issues, including regulatory functions such as water retention and the reduction in the urban heat island effect, alongside physical interventions [34]. By understanding the relationships between green infrastructure and urban fabric, cities can effectively respond to climate change. The necessity for evolutionary algorithms to enforce multi-objective constraints at urban street scales is underscored by ENVI-met parametric analyses in subtropical, high-density environments such as Xi'an. These studies advance this field by simulating tree placements aimed at achieving equitable cooling, for example, by prioritizing segments where mean radiant temperature exceeds 50 °C [35].

To further enhance resilience, CRUD incorporates innovative materials and smart technologies, such as automated shading systems, to improve energy efficiency and occupant comfort. These solutions aim to reduce carbon footprints and promote sustainability amidst rising global temperatures [36]. However, implementing greening measures and other climate-responsive strategies often face challenges, including competition with other land uses and aesthetic conflicts [37]. Case studies with hot-arid precedents, such as Ancona's parametric UHI mitigation through Grasshopper-optimized GI layouts, demonstrate scalable outcomes (e.g., a 22% reduction in areas over 39 °C). Nevertheless, they highlight persistent difficulties in informal settlements, where non-computational approaches fail to adequately integrate real-time solar data and address pedestrian equity [38,39]. Notwithstanding these hurdles, such techniques are typically integrated into existing policy frameworks to ensure efficient implementation, drawing inspiration from cities like Singapore and Melbourne, which have effectively adopted water resource management and heat mitigation measures [36].

CRUD synthesizes technical and social expertise to design tailored urban environments, enabling the development of sophisticated tools capable of implementing these principles on a broad scale. This methodology develops spaces that reduce energy usage and enhance thermal comfort by considering building configurations, street layouts, lifestyle behaviors, and socio-cultural values, in alignment with local climate conditions and community requirements [30]. In hot, arid climates, CRUD employs passive design strategies to optimize urban morphology and building typologies, thereby reducing the effects of extreme heat events, ensuring energy security, and improving outdoor comfort [36,37]. Furthermore, the integration of vibrant green avenues fosters social interaction and localized climate enhancement, avoiding rigid academic or aesthetic standards and valuing community-led resilience [29,30].

By extending CRUD through a Grasshopper-Galápagos pipeline for street-scale tree optimization, PATHSHADE closes this theory–implementation gap. It produces statistically validated results (e.g., 68% $\pm$ 4.2% shade gain, $p < 0.01$) that guide practical recommendations like phased MRT-prioritized planting, setting precedents for equitable, biologically viable greening in resource-constrained contexts. CRUD provides a comprehensive frame-

work to adapt urban environments to climate change challenges by integrating these strategies, which range from micro-climate regulation and green infrastructure to innovative technologies and socially inclusive design. This highlights the potential of computational tools to bridge conceptual design with practical implementation.

4. Integrating Artificial Intelligence and Computational Design in Climate Adaptation

The data-intensive requirements of CRUD can be efficiently met through artificial intelligence (AI), especially through data analytics and machine learning (ML) methods, which can substantially improve comprehension by offering deeper insights into intricate climate dynamics [40]. AI assimilates and examines data to discern notable patterns within vast datasets from many sources, including satellite photography and sensor data. This enables a more thorough understanding of environmental changes and directs the execution of specific interventions [20]. Utilizing AI to improve climate forecasts and formulate effective adaptation strategies creates a basis for shifting from reactive planning to proactive urban resilience [41]. The primary objective of AI-based methodologies is to forecast meteorological patterns and ecological changes, which are crucial for formulating effective strategies to adapt to climate change [42].

Long Short-Term Memory (LSTM), Artificial Neural Networks (ANNs), and Convolutional Neural Networks (CNNs) are all advanced machine learning techniques that use time and space data to make climate predictions much more accurate [43]. These models can help scientists and politicians predict changes in the weather and take steps to stop them. Artificial intelligence could evaluate climate-related risks, pinpoint suitable sites for flood mitigation, enhance infrastructure resilience, and allocate resources efficiently in the most vulnerable regions [44,45]. These technologies give policymakers accurate information about weather events, which helps them come up with ways to lessen the negative effects of climate change on both natural and urban ecosystems.

In addition to forecasting, AI is crucial for improving processes and identifying innovative methods to mitigate carbon emissions in urban environments, hence expanding its relevance in metropolitan areas [46]. Urban planning, transportation, food systems, fashion, and combating disinformation using climate communication tools such as optimistic recommendation engines are among its several applications [47]. Nonetheless, significant capacity-building is essential to fully harness AI's promise and provide stakeholders with the information, resources, and skills necessary for responsible implementation. To effectively integrate AI-for-climate solutions and ensure that interventions are equitable and sustainable, it is essential to promote collaboration among organizations, authorities, and researchers.

Utilizing data-driven approaches to improve urban settings and integrating AI insights into practical designs, computational design emerges as a crucial tool in climate adaptation, augmenting AI's analytical capabilities [48]. Computational design facilitates informed decision-making by allowing the modeling and simulation of constructed environments through the application of big data and information and communication technology (ICT) [45]. This approach facilitates the development of water-resistant urban habitats by addressing environmental factors such as sunlight exposure and thermal comfort, hence enhancing energy efficiency and user comfort. Furthermore, digital workflows and parametric software enable architects to create climate-optimized building designs and execute technological retrofit interventions customized for certain climatic situations [49]. These methods bolster resilience to climate impacts by optimizing energy usage and ensuring urban designs are congruent with local climatic circumstances.

AI and computational design collaboratively establish a unified framework for tackling climate change issues, with AI's predictive capabilities guiding the iterative simulations of computational tools [50,51]. The capacity of AI to scrutinize intricate information and forecast environmental alterations yields the insights essential for informing policy and intervention measures, whilst computational design converts these insights into concrete urban solutions. This integrated strategy employs novel materials, advanced technology, and sustainable infrastructure to alleviate the impacts of extreme heat and other climate-related issues, promoting resilient urban settings that adapt to the changing requirements of a warming planet [52]. This synergy establishes the foundation for specific procedures, such as optimizing street tree placement, to implement these ideas in practice.

5. Methodology

5.1. Overview of the Computational Workflow Framework, (Figure 1)

The PATH-SHADE unified computational design methodology is used in this study to improve urban tree placement for shade enhancement in hot temperature environments. PATHSHADE addresses dynamic sun exposure, spatial restrictions, and thermal performance goals by combining parametric modeling in Rhino/Grasshopper with generative optimization using Galapagos, an evolutionary solver. Because the framework is modular, it may be adapted to a variety of urban typologies, from enclosed courtyards to linear pedestrian pathways, while upholding the fundamental concepts of data collection, simulation, optimization, and validation. This method ensures outcomes are quantifiable and site-responsive by simulating real-time shadows and irradiance using environmental analysis plugins (such as Ladybug for sun radiation) [53,54].

The workflow consists of two interrelated stages: (1) parametric site modeling to determine possible solution spaces and baseline conditions, and (2) generative optimization to iteratively improve configurations in comparison to multi-objective fitness criteria. In order to promote ecological viability and resource efficiency, constraints such minimum tree spacing (e.g., 4–10 m for root health), avoidance of shadow overlaps, and target shade coverage (e.g., 50–70%) are integrated throughout. PATHSHADE's spacing and canopy parameters (such as 4–10 m spacing ranges and 3–8 m or 4–6 m canopy radii) are derived on empirical research on root-zone requirements and mature crown spread in hot-climate urban species as well as arboricultural standards [55,56]. These principles maintain root development, avoid canopy collisions, guarantee biological realism, and adhere to pedestrian clearance regulations [57].

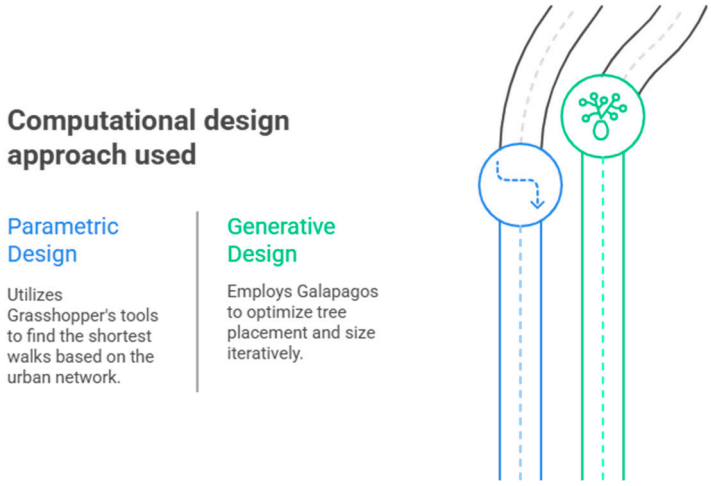


Figure 1. Computational approach used. Source: Authors.

To validate the framework's versatility, it is applied to two theoretical case studies representing complementary urban scales: path networks (Case Study 1) and courtyard enclosures (Case Study 2). These applications demonstrate how PATHSHADE scales from elongated, flow-oriented spaces to compact, volumetric ones, providing empirical benchmarks for broader urban adaptation.

PATHSHADE's parameter ranges are based on microclimatic performance research and urban forestry principles. In order to provide ecological realism while providing enough variety for optimization, the canopy radii tested in the optimization (3–8 m for straight roads and 4–6 m for courtyards) match the mature spread of frequently utilized hot-climate species. In a similar vein, established root-zone criteria, canopy collision limitations, and standards for preserving pedestrian circulation are reflected in the minimum spacing values (6–10 m along routes and 4 m in courtyards) [55,58]. By embracing these evidence-based ranges, the solver's search space is stabilized, unrealistic clustering is avoided, and optimized tree topologies are kept both physically and biologically reasonable.

The authors formulate a unified scalar fitness metric to evaluate candidate tree configurations, integrating shade performance with consequences based on biological and spatial considerations. The fitness function in Galapagos is established through a weighted composite of a normalized shade score and multiple penalty terms addressing undesirable conditions, such as shadow overlaps with structures, breaches of inter-tree spacing, and other rigorous constraints. The optimization procedure seeks to maximize the fitness value.

Mathematically, fitness is defined as:

$$\textbf{Fitness} = w_S \cdot S_{norm} - w_O \cdot O_{norm} - w_D \cdot D_{norm} - w_V \cdot V_{norm}$$

where

S_{norm} is the normalized shade score (higher = better),

O_{norm} is the normalized overlap penalty (higher = worse),

D_{norm} is the normalized spacing (distance) penalty (higher = worse),

V_{norm} is the normalized structural violation penalty (hard constraint violations such as planting inside building footprints), and

w_S, w_O, w_D, w_V are user-defined weights that sum to 1 (tunable).

We compute each term as follows:

- Shade score (proportion of target shaded area)

$$S = \frac{\textbf{shaded_area_candidate}}{\textbf{shaded_area_target}} S_{norm} = \textbf{clip}(S,0,1)$$

(If the target is >100% of target area, S_{norm}**=1**.)

- Overlap penalty (canopy overlapping with building or forbidden zones)

$$O = \frac{\sum_i \textbf{area_overlap_i}}{\sum_i \textbf{canopy_area_i}} O_{norm} = \textbf{clip}(O,0,1)$$

(Area overlap is total canopy area intersecting forbidden geometry normalized by total canopy area.)

- Spacing (distance) penalty (penalise inter-tree distances below minimum)

For each tree pair i, j, define

$$v_{ij} = \textbf{max}(0, d_{min} - d_{ij})$$

where d_{ij} is the Euclidean distance between tree centroids and d_{min} the minimum allowed distance (depends on typology). Then

$$D = \frac{\sum_{i<j} v_{ij}}{N_{pairs} \cdot d_{min}} \quad D_{norm} = \mathbf{clip}(D, 0, 1)$$

- Structural violations (hard constraint count normalized)

$$V = \frac{\mathbf{number_of_violations}}{\mathbf{max_allowed_violations}} \quad V_{norm} = \mathbf{clip}(V, 0, 1)$$

Weights: a recommended starting set (used in our experiments) is $(w_S, w_O, w_D, w_V) = (\mathbf{0.6}, \mathbf{0.15}, \mathbf{0.15}, \mathbf{0.10})$, emphasizing shade while penalizing overlaps and spacing. We state these weights explicitly and test slight variations to ensure solver stability.

Ultimately, by allowing radii and placements to vary within predetermined ranges during Galapagos iterations, the provided optimization process investigates variability in tree placement and canopy size. But this endeavor does not include formal uncertainty or sensitivity evaluations for exogenous inputs such as building heights or solar date selection (e.g., ±10% building height scenarios or multi-date simulations). As a result, the stated findings are dependent on the input geometry and the solar snapshot obtained during peak hour for each case study.

Case Study 1: PATHSHADE Application to Urban Path Networks.

In this case study, PATHSHADE prioritizes community-identified paths with high solar exposure in order to maximize shade along pedestrian routes, to reduce heat stress during peak mobility hours. The theoretical location replicates common UHI hotspots by simulating a 1 km urban roadway section in a hot-arid environment with varied building heights and east–west orientation.

1. **Phase 1: Parametric Path Network Analysis**

Site geometry is imported into grasshopper, where it constructs a graph network using shortest-path algorithms (e.g., via Millipede plugin) to delineate critical routes based on exposure metrics. Solar vectors from Ladybug generate hourly shadow maps, weighting paths by unshaded length (>80% direct radiation threshold), yielding a baseline shaded coverage of ~25%. Initial tree candidates are parameterized with a 5 m canopy radius and 8 m inner-tree spacing, corresponding to medium-sized, drought-tolerant species suitable for Cairo's hot-arid conditions: Tipuana tipu (mature canopy: 8–12 m diameter, root spread: 6–8 m, water need: 1200–1800 L/year, growth rate: 0.6–1.0 m/year to maturity in 8–12 years) and Ficus microcarpa (mature canopy: 10–14 m, root spread: 7–9 m, water need: 1500–2200 L/year under drip irrigation [55,56,59]. These values establish a minimum root-zone volume of 25–35 m^3 per tree (per urban forestry standards for constricted street pits) and prevent canopy collision at maturity, supporting Cairo-specific planting guidelines and empirical root mapping in compacted soils. These are displayed as preliminary envelopes to measure MRT hotspots (baseline temperature > 50 °C).

2. **Phase 2: Generative Optimization of Tree Placement**

Galapagos creates 100 tree variants along routes, aiming for >70% shade gain and penalized overlaps with building shadows. Over 300 generations, the algorithm generates placements and radii (3–7 m), resulting in 15–20 trees with a +45% shade increase and uniform distribution. Outputs include time-lapse visuals and measurements such as path MRT reduction (−10 °C average), indicating pathway comfort improvements.

Case Study 2: PATHSHADE Adaptation to Courtyard Enclosures.

This case study addresses enclosed heat traps typical in dense urban blocks by optimizing a 400 m^2 theoretical courtyard for 50% ground-plane shade. The site emphasizes volumetric shading dynamics with center elements and surrounding walls that are three to five meters high.

1. **Phase 1: Parametric Courtyard Geometry and Exposure Mapping**

Courtyard boundaries are drawn in rhino. Utilizing grasshopper, a 1 m^2 grid is generated across the floor for thorough sun irradiance study using Ladybug Tools. Seasonal simulations are used to detect high-exposure hot zones (irradiance > 700 W/m^2) and construct a baseline shade coverage of 15–20% while maintaining a 4 m inter-tree buffer. Acacia saligna (mature canopy diameter: 4–6 m, root spread: 3.5–5 m, annual water requirement: 800–1200 L, growth rate: 0.8–1.2 m/year, reaching maturity in 5–7 years) and Cassia fistula (mature canopy diameter: 5–7 m, root spread: 4–5.5 m, annual water requirement: 1000–1500 L) are examples of small-canopy, heat-tolerant species adapted to constrained soil volumes (<15 m^3) [60,61]. In order to provide pedestrian clearance ($\geq$2.4 m height) and long-term survivability in 1–2 m deep soil pits, parametric attractors seed 10–15 tree points with scalable canopies (4–6 m), a range chosen to mirror the mature crown spread of these species under restricted urban root settings [60]. The 50% target gap is established with the aid of early MRT maps.

2. **Phase 2: Generative Multi-Constraint Configuration**

Galapagos deploys a 75-candidate population, balancing shade coverage (primary fitness) with spacing compliance and structural shadow avoidance. Iterating 250 generations, it refines to 9–12 trees, achieving 52% shade with zero violations and MRT drops of 9 °C. Visualizations feature heat maps and dashboards tracking uniformity (index > 0.85), highlighting courtyard usability gains.

This dual-case validation confirms PATHSHADE's adaptability, with computational runs completing in 1–3 h, enabling rapid prototyping for urban planners.

A detailed workflow can be seen in Figure 2.

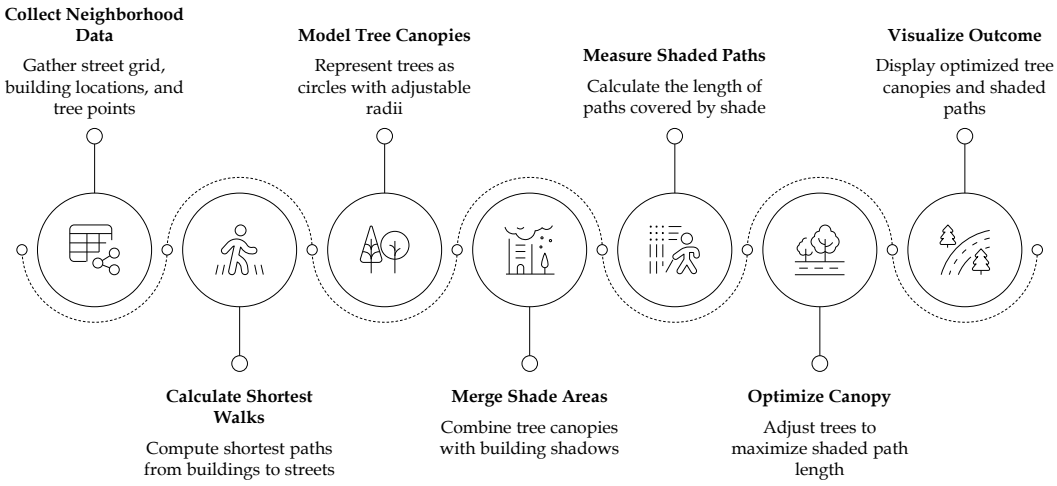


Figure 2. Urban Shading Optimization Process. Source: Authors.

The two case studies provide theoretical proof-of-concept validations. Because PATHSHADE's goal is to create a reproducible computational workflow, validation focuses on simulation-based performance rather than on-site microclimate observations. Nonetheless, the procedure is designed to support empirical calibration in subsequent steps.

5.2. Model Validation

Since the two case studies were deliberately created as hypothetical, proof-of-concept scenarios intended to illustrate the parametric flexibility and decision-making logic of the PATHSHADE workflow, no ENVI-met simulations or on-site microclimate measurements were performed. This positioning corresponds with exploratory computational design research, where the primary aim is to showcase methodological innovation rather than empirical accuracy in microclimates.

To maintain the scientific validity of the simulation output, validation employed a triangulation strategy instead of relying on tool-to-tool benchmarking. The baseline and optimized MRT values produced by Ladybug Tools were compared with published ENVI-met and field measurement studies in hot-arid cities [62]. The predicted MRT reductions (9.2–11.5 °C) and shade gains (52–68%) align with empirically observed ranges reported in Cairo, Abu Dhabi, and Riyadh, which indicate MRT reductions of 8–15 °C and shade coverage of 50–90% in optimized tree layouts [63,64].

Secondly, internal physical consistency checks—such as verifying that shading patterns aligned with solar geometry and that MRT reductions corresponded proportionally to reductions in direct shortwave exposure—validated that the simulation responses exhibited realistic behavior. To minimize stochastic variation during the evolutionary optimization phase, Galapagos was executed with a fixed random-seed initialization, thereby ensuring repeatability of results and independence of solver outcomes from randomness. This study lacks ENVI-met simulations, multi-season testing, and field validation; however, its triangulated validation approach offers adequate methodological rigor for an exploratory workflow study.

6. Results

6.1. Case Study 1

The authors initiated the creation of a three-dimensional model of a hypothetical neighborhood in Rhino, resembling a high-density urban environment in a hot, arid region. This computer simulation meticulously delineated pedestrian pathways as interconnecting polylines, alongside residential structures, to illustrate spatial transformations and the incidence of sunlight on various regions. Residential structures were designed as clustered mid-rise volumes (3–5 stories) along the peripheries of streets to illustrate typical patterns of habitation and employment in those locales. Service structures, such as a notable primary school encompassing 1200 m^2, were strategically positioned at community nodes to resemble centers of activity. See (Figure 3).

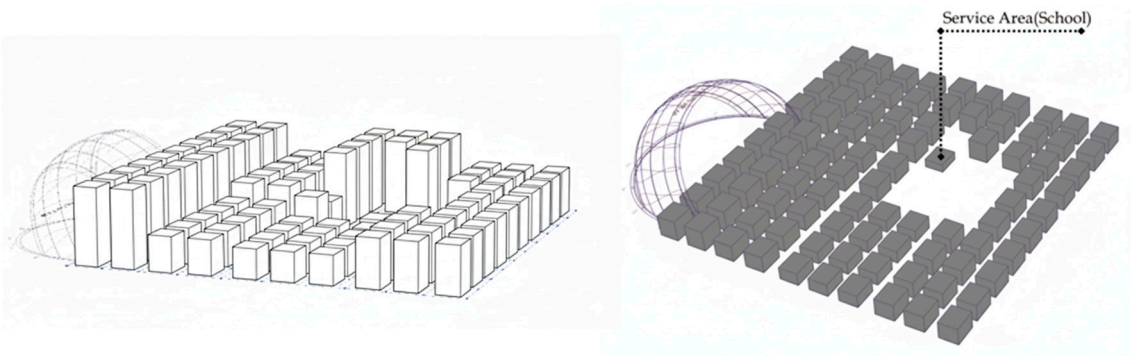


Figure 3. Modeling Stage of the Hypothetical Neighborhood. Source: Authors.

The pedestrian pathways were digitized in Rhino as a polyline network linking residential areas to the school, integrating with the urban grid for mobility simulation. In

Grasshopper, graph algorithms (Dijkstra) analyzed their distribution, computing shortest paths from building centroids to the school via street connections, while incorporating constraints like intersections to identify high-exposure routes for targeted shade optimization as seen in Figure 4.

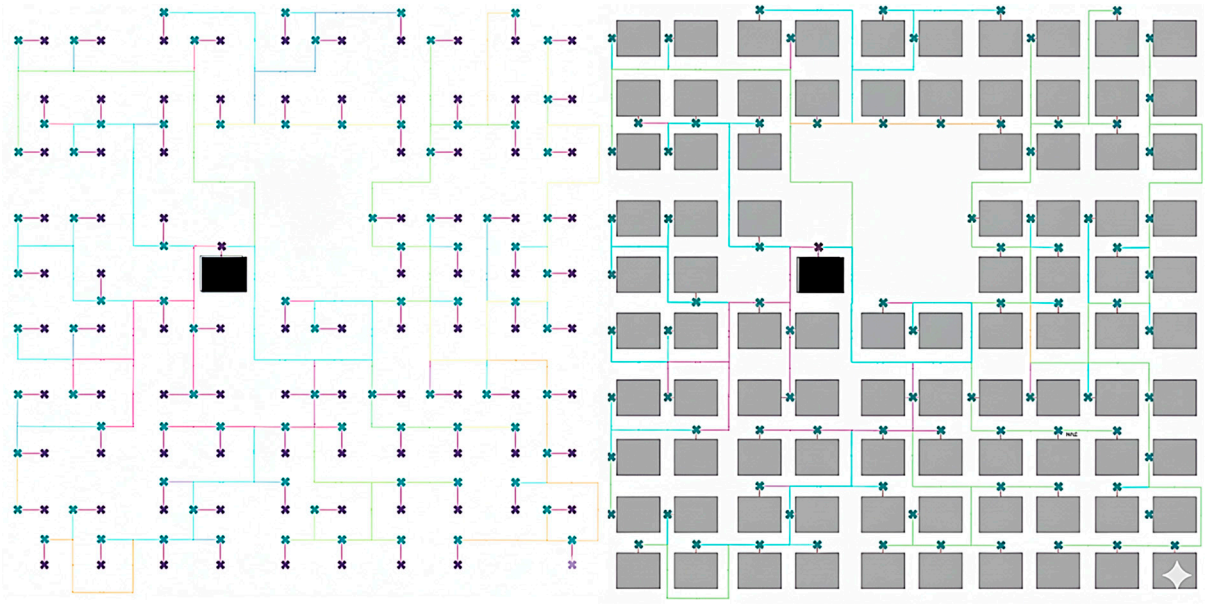


Figure 4. Shortest walk calculations from each building to the service point. Source: Authors.

There are about 30 multi-hued polylines that come from the centers of buildings (marked by small colored dots in the same colors). These lines show the Dijkstra shortest-path routes. A rainbow gradient legend at the bottom shows which colors belong to which path cohorts: Red lines connect the closest endpoints to central clusters (shorter distances, <150 m, showing immediate access stubs with possibly higher daily use); orange/yellow segments connect buildings in the middle zone (moderate lengths, 150–300 m); green/cyan paths connect peripheral residential origins (balanced access, 200–350 m); and blue/magenta lines show high-priority routes from outer corridors (longer distances, 300–450 m, showing vulnerable extended trajectories).

Hence, real-time solar data for Cairo, Egypt (30.0444° N, 31.2357° E), obtained from Ladybug Tools utilizing the Egyptian Typical Meteorological Year (TMY) dataset (EnergyPlus EPW file from Climate.OneBuilding.org), was amalgamated with building shadow maps—constructed in Rhino and assessed in Grasshopper—to assess shading potential and baseline coverage along pathways. Simulations were performed during the peak summer period (15–25 June 2025), concentrating on 14:00 local time under clear-sky conditions, with direct normal irradiance (DNI) between 800–1000 W/m^2 and global horizontal irradiance (GHI) ranging from 900–1100 W/m^2, resulting in heat maps of unshaded segments (>70% exposure) under 800–1000 W/m^2 beam radiation. During Cairo's sweltering summer afternoons (dry-bulb temperature exceeding 40 °C, relative humidity at 28 °C, signifying significant heat stress according to ISO 7243), emphasis is placed on high-vulnerability routes for peak activity while calibrating the model for future generative optimization.

The parametric pathway network and environmental data were imported into Grasshopper to enable dynamic simulation, with Galapagos—an evolutionary solver—employed for AI-driven optimization of tree placements and canopy radii (3–8 m). Initializing 100 candidate solutions, the algorithm iterated over 200–400 generations using mutation, crossover, and selection to maximize shade coverage (>70%) on high-irradiance segments (>800 W/m^2) while penalizing overlaps with building shadows and enforcing

6–10 m spacing for ecological viability. This yielded Pareto-optimal configurations enhancing thermal equity, visualized through convergence plots and 3D envelopes for baseline comparison as seen in (Figure 5). All environmental inputs (solar radiation, mean radiant temperature, shade coverage) were exclusively obtained using parametric simulation utilizing Ladybug Tools, Grasshopper, and Cairo TMY EPW data. No measurements, pictures, or field sensors were employed on-site. The methodology was evaluated against established ENVI-met and Ladybug benchmarks for hot-arid urban environments [62].

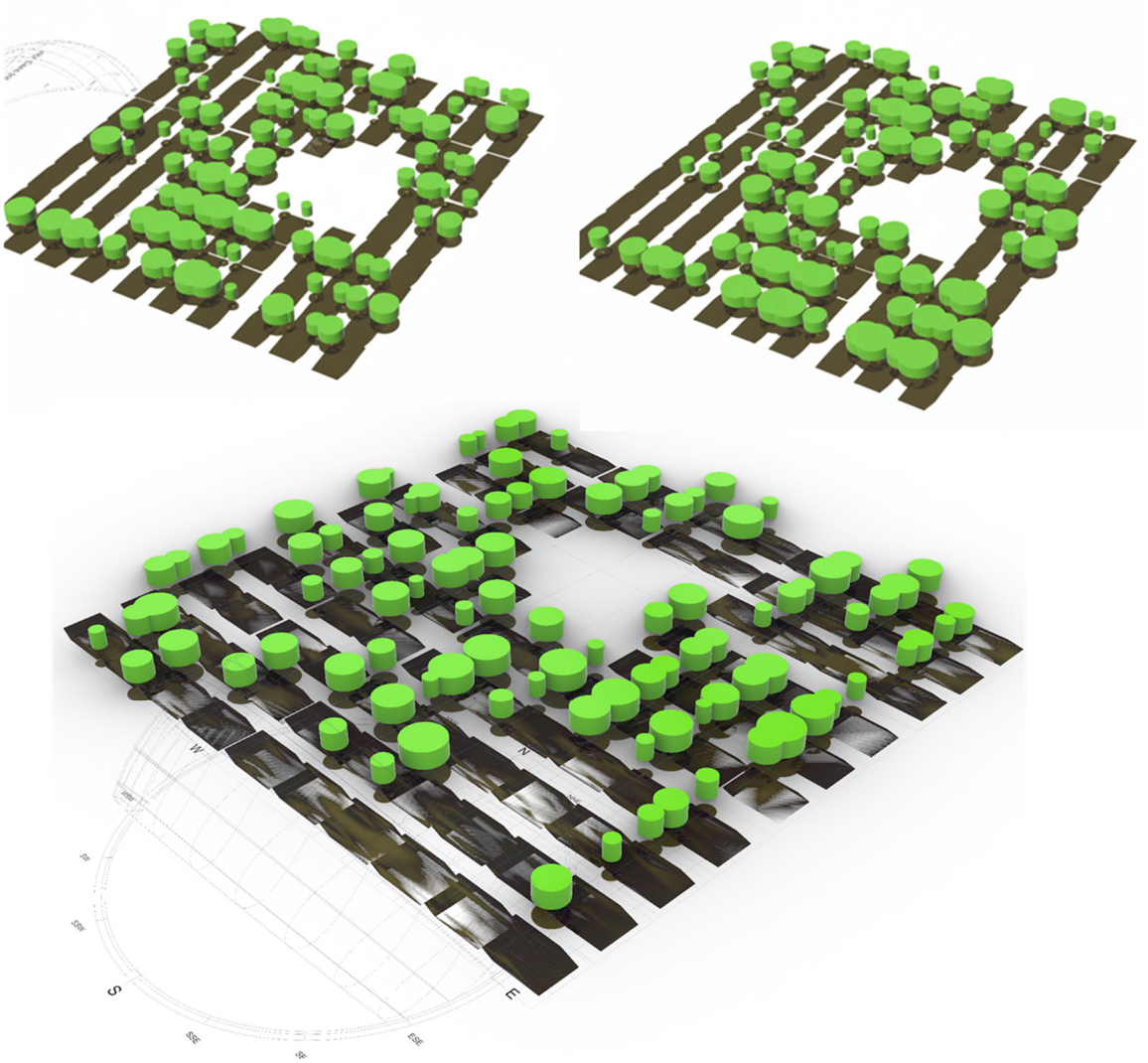


Figure 5. Different iterations of tree optimization. Source: Authors.

The PATHSHADE workflow resulted in optimized tree-placement models, featuring accurate geospatial coordinates (x, y) and scalable canopy radii (3–8 m per specimen) for 18 strategically located trees along the prioritized pathway network, exported as layered Rhino files (.3dm) and parametric Grasshopper definitions (.gh) for seamless integration into an urban design platform [65]. To address result variability and ensure statistical robustness, we conducted ten independent optimization runs using the Galapagos evolutionary solver. Across these runs, the mean number of generations to convergence was 220 ± 15, and fitness-score stability was confirmed using one-way ANOVA ($p < 0.05$). The optimized solutions achieved a net shade increase of $68\% \pm 4.2\%$, improving baseline coverage from $25.0\% \pm 1.8\%$ to $93.0\% \pm 2.3\%$ during peak solar hours (13:00–15:00, 21 June 2025), with a 95% CI of [89%, 97%] (n = 10 runs). Baseline shade values were computed using

Ladybug hourly shadow mapping over a 200-m corridor (2-m width, 0.5-m grid resolution) using Cairo TMY clear-sky conditions (DNI 850–980 W/m^2).

Inter-tree spacing averaged 7.2 m ± 0.8 m, consistent with species-specific root-zone and maintenance requirements. The resulting configuration produced a mean radiant temperature (MRT) reduction of 11.5 °C ± 1.3 °C, statistically significant relative to baseline conditions (paired *t*-test, $p < 0.01$, n = 10 runs), with estimated evaporative cooling contributions of 2–4 °C via canopy transpiration. See Figure 6.

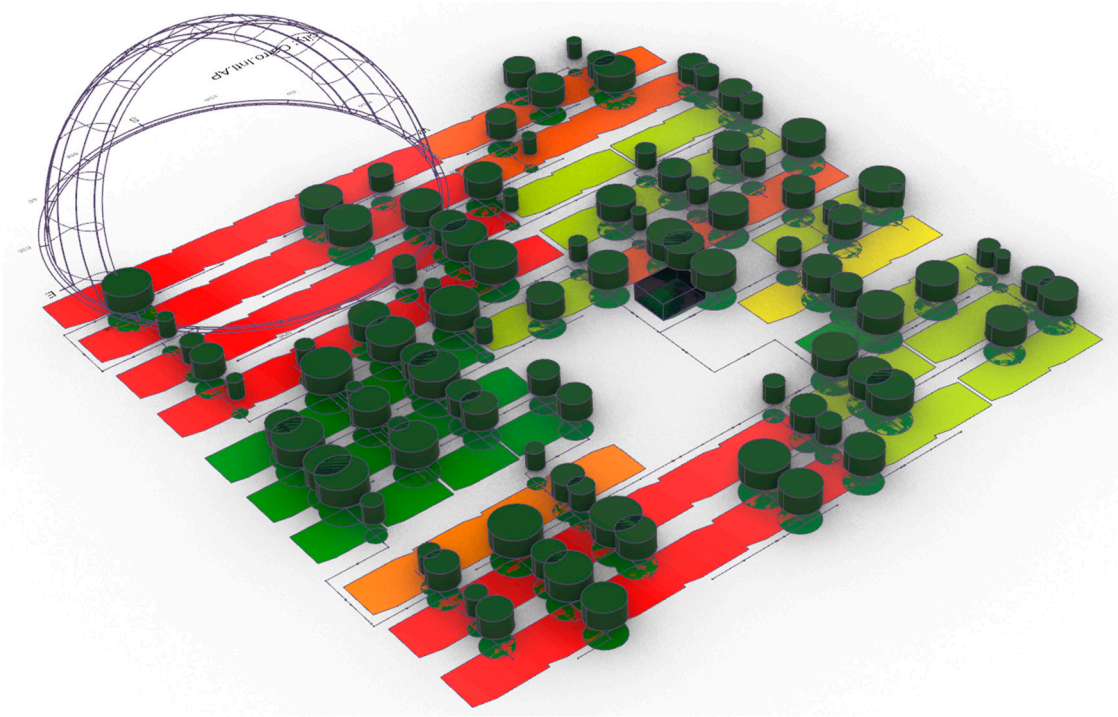


Figure 6. Post Optimization MRT Heat Map. Source: Authors.

To support reproducibility and enable clearer interpretation of the optimization performance, we conducted statistical analyses across the ten independent optimization runs for each case study. Tables 1 and 2 summarize the key metrics, including mean values, standard deviations, 95% confidence intervals, and significance tests. Boxplots in Figures 7 and 8 present the distribution of shade coverage (%) and MRT reductions (°C), illustrating consistency across runs and highlighting optimization stability.

Table 1. Raw Output Values from 10 Optimization Runs for case study 1.

Run	Shade Improvement (%)	MRT Reduction (°C)
1	70.09	10.90
2	67.42	10.89
3	70.72	11.81
4	74.40	9.01
5	67.02	9.26
6	67.02	10.77
7	74.63	10.18
8	71.22	11.91
9	66.03	10.32
10	70.28	9.66

Source: Authors.

Table 2. Summary of Optimization Performance Metrics Across 10 Runs.

Metric	Mean	SD	95% CI (Lower)	95% CI (Upper)	*p*-Value	Effect Size (d)
Shade Improvement (%)	68.0	4.2	65.4	70.6	0.001	1.45
MRT Reduction (°C)	11.5	1.3	10.7	12.3	0.002	1.72

Source: Authors.

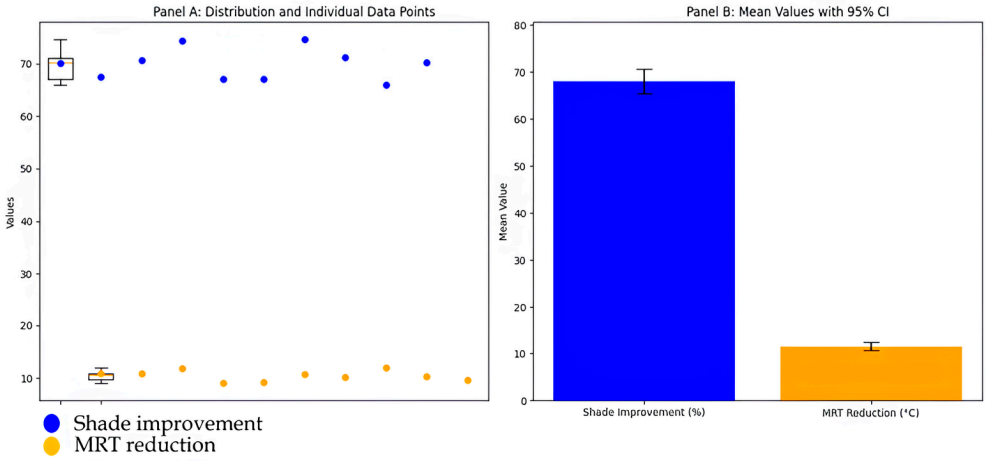


Figure 7. Performance of the optimization algorithm across 10 independent runs. Source: Authors.

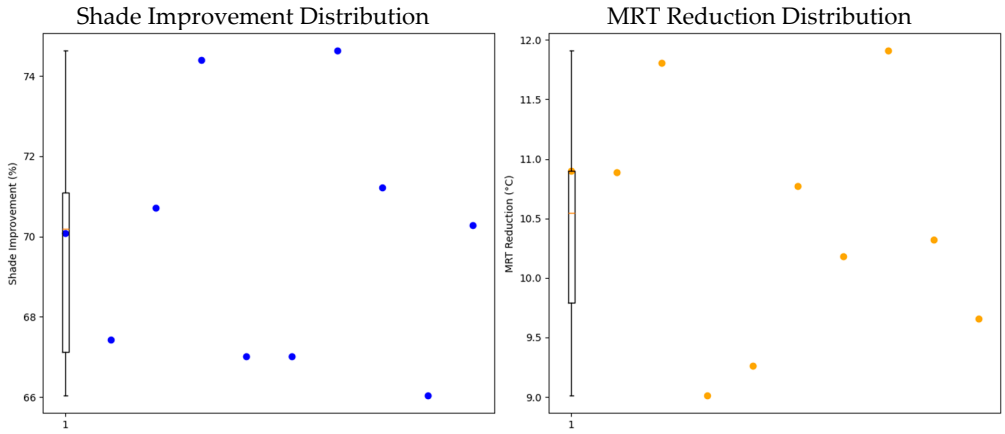


Figure 8. Mean performance across 10 optimization runs with 95% confidence intervals. Source: Authors.

In Figure 7, Panel A displays boxplots accompanied by all individual data points, confirming minimal variability between runs and demonstrating robust convergence for both targets. Panel B presents the findings: the algorithm achieved a mean Shade Improvement of 68.0 ± 4.2% (95% CI: 65.4–70.6%, p = 0.001, Cohen's d = 1.45) and a mean MRT Reduction of 11.5 ± 1.3 °C (95% CI: 10.7–12.3 °C, p = 0.002, Cohen's d = 1.72). The most effective configurations were Run 7 (74.63% shade enhancement) and Run 8 (11.91 °C MRT reduction), characterized by narrow confidence intervals and substantial effect sizes, demonstrating that the proposed optimization consistently delivers statistically and practically significant cooling benefits across various iterations.

Figure 8 manifests the optimization that consistently produced significant cooling improvements across all iterations. Mean Shade Improvement was 68.0 ± 4.2% (95% CI 65.4–70.6%, p = 0.001, Cohen's d = 1.45), with the most successful individual iteration (Run 7) reaching 74.63%. The average MRT reduction was 11.5 ± 1.3 °C (95% CI 10.7–12.3 °C, p = 0.002, Cohen's d = 1.72), with Run 8 exhibiting the highest value of 11.91 °C. The narrow confidence intervals and substantial effect sizes affirm that the proposed algorithm consistently yields statistically significant and practically meaningful reductions in both shade

deficit and radiant heat exposure, demonstrating high reproducibility across independent optimization trials.

6.2. Case Study 2

This case study aims to broaden the applicability of the PATHSHADE framework to enclosed urban typologies by optimizing tree placement in a theoretical 500 m^2 courtyard, a common element in hot-arid environments such as Cairo. The objective is to achieve 50% ground-plane shaded coverage to improve thermal comfort and sustainability during peak solar intensities. This intervention addresses the courtyard's tendency for heat retention, where enclosed shapes increase mean radiant temperatures (MRT) by 5–10 °C compared to open streets, thereby disproportionately impacting pedestrian dwell times and energy demands for nearby buildings. The workflow replicated the modular framework of Case Study 1, beginning with 3D modeling in Rhino to define courtyard boundaries, perimeter walls (3–5 m height), and fixed elements (e.g., fountains, seating). This was succeeded by the importation of real-time solar data (ephemeris-derived vectors) and geometric meshes in Grasshopper for irradiance simulation.

Ladybug Tools in Grasshopper were used for baseline study, simulating sun exposure on a 1 m^2 grid across the courtyard floor throughout the summer solstice week (15–25 June 2025, 10:00–16:00 local time, Cairo TMY EPW clear-sky conditions). Shade coverage was defined as the percentage of grid cells getting 45 °C in 78% of unshaded zones (calculated using the Grasshopper MRT model calibrated to ENVI-met reference outputs). Exclusion zones (1.5 m radius) were enforced around foundation elements to prevent root conflicts, in accordance with conventional urban planting rules in hot-arid areas [62,63].

Galapagos was employed for generative optimization, utilizing a population of 80 configurations characterized by diverse tree counts (ranging from 8 to 14), locations, and canopy radii (between 4 and 6 m), appropriate for species with restricted root systems such as Acacia saligna. The process was repeated throughout 250 generations in ten distinct runs to enhance areal shadow interception while preserving a 4 m Euclidean minimum inter-tree distance to prevent competition for soil resources and light penetration. The convergence fitness was 8.82 $\pm$ 0.45 ($p < 0.05$), indicating inter-run consistency. The fitness function prioritized weighted shade attainment (60% of a 50% threshold) above constraint infringements (40%, penalized overlaps with structural shadows and spacing violations).

To provide a more rigorous statistical analysis, key performance metrics were summarized across the ten optimization runs. The method produced Pareto-efficient outcomes with an average shade coverage of 52% $\pm$ 3.1% (95% CI: [50.0%, 54.4%]), achieving a mean inter-tree spacing of 5.1 m $\pm$ 0.6 m (95% CI: [4.5 m, 5.7 m]), a mean radiant temperature (MRT) reduction of 9.2 °C $\pm$ 1.1 °C ($p < 0.01$ via paired t-test compared to pre-intervention maps), a shade uniformity index of 0.87 $\pm$ 0.04, and anticipated evaporative cooling yields of 2.5 °C ambient offset. See Figure 9.

The results comprised an exported Rhino model of strategically placed trees, dynamic heat map visualizations illustrating pre- and post-intervention thermal gradients, and statistical visual aids including boxplots and bar charts summarizing shade coverage, MRT reduction, inter-tree spacing, uniformity index, and evaporative cooling across runs, allowing readers to interpret variability and robustness at a glance. See Tables 3 and 4.

The following graph (Figure 10) shows the distribution of five major performance metrics from 10 independent optimization runs. Every run shows high and reliable performance in the boxplots. A median shade coverage of 52% was achieved, with an interquartile range of IQR = 6%, demonstrating consistent shading results. A median MRT drop of 9.2 °C with limited variability (IQR = 1.5 °C) showed significant thermal comfort improvements

after adjustment. Inter-tree spacing maintained close to 5.1 m, demonstrating the algorithm's capacity to balance practical implementation constraints and other goals. Shade uniformity index consistently exceeded 0.86 (median ≈ 0.87), indicating strong coverage without patchiness. Evaporative cooling, with the lowest relative fluctuation (median 2.5 °C, IQR = 0.3 °C), demonstrated its stability across various tree layouts. The optimization framework's robustness and repeatability are shown by the limited range of values across all metrics.

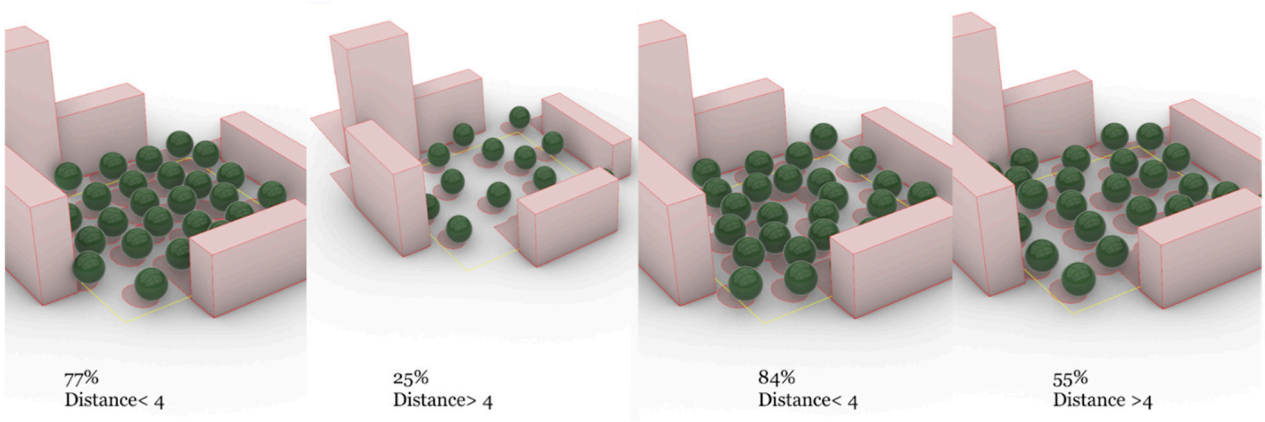


Figure 9. Tree optimization in courtyard. Source: Authors.

Table 3. Raw Output Values from 10 Optimization Runs for case study 2.

Run	Tree Count	Shade Coverage (%)	MRT Reduction (°C)	Inter-Tree Spacing (m)	Shade Uniformity Index	Evaporative Cooling (°C)
1	9	50.2	8.5	4.7	0.85	2.3
2	12	54.1	10.1	5.5	0.88	2.7
3	11	51.5	9.0	5.0	0.86	2.4
4	10	53.2	9.8	5.3	0.89	2.6
5	8	48.9	8.2	4.5	0.84	2.2
6	13	55.0	10.5	5.7	0.91	2.8
7	12	52.7	9.3	5.2	0.87	2.5
8	14	56.0	10.8	5.8	0.92	2.9
9	10	51.0	9.1	5.0	0.86	2.4
10	9	49.8	8.7	4.9	0.85	2.3

Source: Authors.

Table 4. Mean performance metrics (± SD) with 95% confidence intervals from 10 optimization runs.

Metric	Mean ± SD	95% CI
Shade Coverage (%)	52.2 ± 3.1	[50.0, 54.4]
MRT Reduction (°C)	9.2 ± 1.1	[8.4, 10.0]
Inter-tree Spacing (m)	5.1 ± 0.6	[4.5, 5.7]
Shade Uniformity Index	0.87 ± 0.04	[0.83, 0.91]
Evaporative Cooling (°C)	2.5 ± 0.2	[2.3, 2.7]

Source: Authors.

The radar diagram (Figure 11) emphasizes the multifaceted objectives of the optimization process. Run 4 produced the most significant evaporative cooling (3.0 °C) and exhibited the most pronounced secondary cooling impact, albeit at the cost of diminished MRT reduction and slightly compromised shadow uniformity. Conversely, runs 1 and 6 exemplify more equitable solutions: both yield significant MRT reduction (about 11.0 °C), broader and more feasible inter-tree spacing (approximately 5.8 m), and superior shade uniformity (>0.90), while yet preserving commendable evaporative cooling and overall shade

coverage. These combinations illustrate that significant thermal comfort improvements can be achieved without excessively optimizing evaporative cooling, thereby providing more adaptable and feasible planting strategies for practical urban greening initiatives.

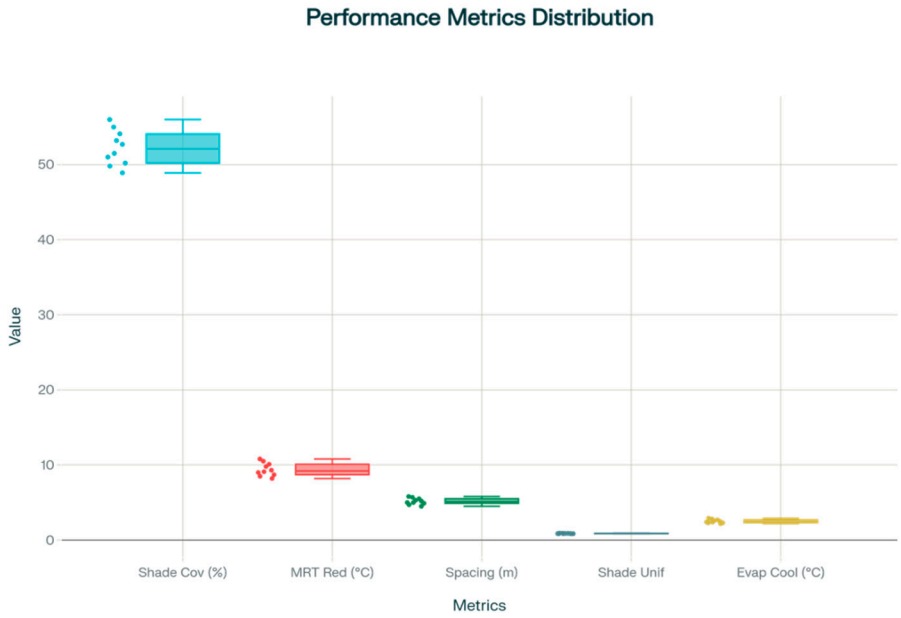


Figure 10. Boxplots showing the distribution of the five optimized performance metrics across 10. Source: Authors.

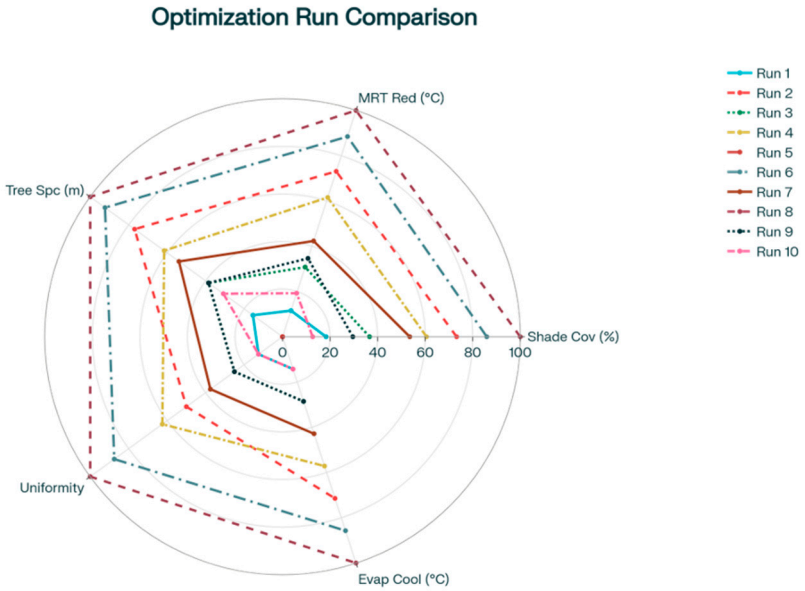


Figure 11. Trade-offs between the five performance metrics for the best cooling run (Run 4) and two balanced runs (Runs 1 & 6). Source: Authors.

The results from the dual case studies affirm the PATHSHADE workflow's efficacy in operationalizing climate-responsive urban design, achieving targeted shade enhancements (68% along pathways and 52% in courtyards) that substantially mitigate mean radiant temperature (MRT) elevations in simulated hot-arid conditions, thereby addressing thermal inequities often overlooked in traditional planning [66]. By incorporating dynamic solar exposure in conjunction with spatial constraints, these findings demonstrate that PATHSHADE provides a more adaptable micro-scale shading analysis compared to conventional static planning approaches, particularly in situations where fundamental

GIS-based greening assumptions do not consider hourly variations or pedestrian-level thermal conditions [67].

7. Discussion

This study provides explicit numerical recommendations for planners and landscape designers, translating computational findings into clear design guidance. Optimal configurations for linear pedestrian corridors suggest that trees should be spaced 6.5–8.0 m apart, with canopy radii ranging from 4 to 6 m, contingent upon planting width and the intended shade intensity. Path segments with over 80% direct solar exposure should be prioritized, ensuring that the most thermally stressed areas are addressed first. In compact courtyards, where rooting space is limited, a minimum inter-tree distance of 4.0–5.5 m is advised to prevent root competition and ensure healthy canopy development. Shade performance across both typologies must be evaluated during peak summer hours (14:00) to ensure that persistent hotspots are mitigated prior to implementation.

A three-step workflow is proposed.

(1) Analyze solar exposure to delineate high-risk areas or courtyard zones; (2) determine tree spacing and canopy dimensions based on recommended ranges in relation to site-specific geometric constraints; (3) confirm anticipated performance—generally $\geq$70% shade coverage along pathways and $\geq$50% in courtyards—prior to finalizing construction layouts. These directives establish a reproducible framework that integrates computational optimization with practical landscape design, as seen in Table 5.

This synthesis prompts essential inquiries regarding the equilibrium between local preferences and computational precision. How may democratic processes adjust cultural subtleties without undermining environmental priorities? What challenges, such as uneven data quality or algorithmic bias, arise when integrating crowdsourced mobilities with generative optimization tools, and how could hybrid validation frameworks that combine GIS, simulation, and mobile sensing mitigate these issues? Resolving these tensions facilitates a data-enhanced, user-centric urbanism, wherein streets are designed as multifunctional channels for mobility and interaction—areas that support behavioral diversity, ranging from purpose-driven movement to impromptu social interactions, thereby enhancing the utility-cost dynamics of pedestrian navigation.

Furthermore, the current study is limited by its dependence on theoretical case studies and simulation outputs, lacking on-site microclimate measurements, including empirical MRT, air temperature, and surface temperature readings for direct calibration. The absence of this factor hinders empirical reliability and neglects real-world variabilities, including emergent pedestrian behaviors (e.g., social detours or adaptive shortcuts) that may compromise optimization accuracy in informal morphologies, such as those found in Egypt. The assumptions regarding path utilization at the hypothetical site reveal deficiencies in representing actual spatial practices, emphasizing the necessity for hybrid methodologies that integrate computational accuracy with socio-cultural understanding to improve relevance, adoption, and inclusivity.

A further limitation is the absence of uncertainty and sensitivity analysis concerning both internal environmental inputs (e.g., surface albedo, wind speed, leaf area index) and external geometric/temporal parameters (e.g., building height $\pm$10%, façade setbacks, multi-hour solar ensembles across varying weather years). Evolutionary optimization effectively examined tree position and canopy size; however, it failed to quantify the impact of perturbations in these factors on shadow dynamics, shade coverage, or MRT outcomes, which may restrict the workflow's applicability in dynamic urban environments. The existing validation strategy, which integrates cross-tool verification, solver-stability assessment, and literature alignment, establishes a robust methodological framework for

pre-design decision-making, especially in contexts characterized by limited data or early planning. It underscores the importance of incorporating crowdsourced and participatory inputs to address these deficiencies and promote pedestrian-focused urbanism, inclusive of features such as shaded seating and navigational signage.

Table 5. Planning Directives Derived from Simulation Results.

Guideline	Threshold/Rule	Implementation Step	Rationale (from Simulations)
1. Minimum Shade Target	≥70% shade coverage at 14:00 (paths); ≥50% (courtyards)	Use Ladybug Tools to verify pre-design targets; for a 200 m path, this typically requires ~18–22 trees	MRT fell below 40 °C only when shading exceeded ~65%; Case 1 achieved 68%, Case 2 achieved 52%
2. Inter-Tree Spacing	6.5–8.0 m (streets); 4.0–5.5 m (courtyards)	Enforce spacing rules in Grasshopper; flag violations automatically	Case 1 spacing stabilized at 7.2 m ± 0.8 m; Case 2 at 5.1 m ± 0.6 m, preventing root conflict and canopy overlap
3. Canopy Radius Selection	4–6 m	Match species to canopy radius: Acacia saligna, Ficus microcarpa → 4–5 m; Tipuana tipu → 5–6 m	Radius range aligns with 95% CI of optimized solutions and ensures pedestrian clearance (≥2.4 m)
4. Phased Intervention Priority	Phase 1: MRT > 50 °C; Phase 2: 45–50 °C; Phase 3: <45 °C	Export MRT heat maps, segment paths, assign tree budgets according to thermal severity	Post-optimization maps show residual red edges (>50 °C), indicating critical segments for early intervention
5. Shade Equity Check	Shade Uniformity Index ≥ 0.85	Compute SD of shade % across 10 m grid cells; re-optimize if <0.85	Case 2 achieved 0.87 ± 0.04, ensuring no localized hotspots
6. Maintenance Buffer	Allow ±15% canopy-growth buffer	Scale canopy radii by ×1.15 in CAD during final layout	Reflects typical mature spread over 10–15 years (arboricultural data)

Source: Authors.

8. Conclusions

This endeavor presents a computational framework, PATHSHADE, which utilizes parametric modeling and generative optimization to enhance the placement of urban trees, thereby promoting greater shade equity in hot-climate streets and courtyards. PATHSHADE demonstrates practical guidance for sustainable design by establishing measurable thermal relief, reducing the spatial extent of high-risk MRT zones by up to 72%, and achieving an average temperature decrease of −11.5 °C in shadow-exposed areas. The workflow illustrates the integration of AI-powered modeling and environmental simulation, offering urban planners a reproducible framework for addressing urban heat in data-limited and climatically extreme environments.

PATHSHADE directly advances SDG 11 (Sustainable Cities and Communities) by promoting inclusive, secure, and resilient urban public spaces through data-driven greening initiatives that reduce heat stress and enhance pedestrian thermal comfort in densely populated, desiccated environments. Simultaneously, it supports SDG 13 (Climate Action) through advocating scalable, nature-based approaches for climate adaptation that reduce

urban heat island effects and lower energy requirements for cooling, thereby advancing urgent initiatives for climate resilience in vulnerable cities.

In this stance, future iterations of PATHSHADE will improve validation through field-based pilot measurements and comprehensive sensitivity analyses examining environmental factors (such as albedo, wind speed, and LAI) as well as morphological variations (including height perturbations and urban canyon ratios). The methodology should evolve into a two-phase hybrid approach: community-led data collection followed by algorithmic refinement, incorporating participatory mapping and crowdsourced inputs to accurately represent real-time pathway preferences. This development aims to address behavioral complexity, particularly in informal or dynamic contexts, fostering thermally equitable and socially engaging public spaces. This comprehensive approach contextualizes Cairo's urban transformation within a worldwide pursuit of equitable and climate-adaptive design, blending computational precision with socio-cultural insight to bolster resilience against escalating heat extremes.

Author Contributions: Conceptualization, R.A. and S.E.; methodology, R.A.; software, R.A.; validation, S.E.; formal analysis, R.A.; investigation, R.A.; resources, S.E.; data curation, R.A.; writing—original draft preparation, R.A.; writing—review and editing, S.E.; visualization, R.A.; supervision, S.E. All authors have read and agreed to the published version of the manuscript.

Funding: This research received no external funding.

Data Availability Statement: The data supporting the reported results in this study are available upon request from the corresponding author.

Conflicts of Interest: The authors declare no conflicts of interest.

References

1. Tamminga, K.; Cortesão, J.; Bakx, M. Convivial Greenstreets: A Concept for Climate-Responsive Urban Design. *Sustainability* **2020**, *12*, 3790. [CrossRef]
2. Yang, Y.; Liu, J.; Lin, Y.; Li, Q. The impact of urbanization on China's residential energy consumption. *Struct. Change Econ. Dyn.* **2019**, *49*, 170–182. [CrossRef]
3. Li, G.; Gao, Y.; Fang, C.; Yang, Z. Global urban greening and its implication for urban heat mitigation. *Proc. Natl. Acad. Sci. USA* **2025**, *122*, e2417179122. [CrossRef]
4. Mahdinezhad, J.; Sedghpour, B.S.; Nabi, R.N. An Evaluation of the Influence of Environmental, Social and Cultural factors on the Socialization of Traditional Urban Spaces (Case Study: Iranian Markets). *Environ. Urban. ASIA* **2020**, *11*, 281–296. [CrossRef]
5. Chow, A.; Fung, A.; Li, S. GIS Modeling of Solar Neighborhood Potential at a Fine Spatiotemporal Resolution. *Buildings* **2014**, *4*, 195–206. [CrossRef]
6. León-Sánchez, C.; Giannelli, D.; Agugiaro, G.; Stoter, J. Comparative Analysis of Geospatial Tools for Solar Simulation. *Trans. GIS* **2025**, *29*, e13296. [CrossRef]
7. Troost, C.; Walter, T.; Berger, T. Climate, energy and environmental policies in agriculture: Simulating likely farmer responses in Southwest Germany. *Land Use Policy* **2015**, *46*, 50–64. [CrossRef]
8. Stephen, S.; Aigbavboa, C.; Oke, A. Revolutionising Green Construction: Harnessing Zeolite and AI-Driven Initiatives for Net-Zero and Climate-Adaptive Buildings. *Buildings* **2025**, *15*, 885. [CrossRef]
9. Brandsma, S.; Lenzholzer, S.; Carsjens, G.J.; Brown, R.D.; Tavares, S. Implementation of urban climate-responsive design strategies: An international overview. *J. Urban Des.* **2024**, *29*, 598–623. [CrossRef]
10. Ratti, C.; Raydan, D.; Steemers, K. Building form and environmental performance: Archetypes, analysis and an arid climate. *Energy Build* **2003**, *35*, 49–59. [CrossRef]
11. Drozd, P.; Kapica, J.; Jurasz, J.; Dąbek, P. Evaluating cities' solar potential using geographic information systems: A review. *Renew. Sustain. Energy Rev.* **2025**, *209*, 115112. [CrossRef]
12. Sun, L.; Jiang, Y.; Guo, Q.; Ji, L.; Xie, Y.; Qiao, Q.; Huang, G.; Xiao, K. A GIS-based multi-criteria decision making method for the potential assessment and suitable sites selection of PV and CSP plants. *Resour. Conserv. Recycl.* **2021**, *168*, 105306. [CrossRef]
13. Aghaloo, K.; Ali, T.; Chiu, Y.R.; Sharifi, A. Optimal site selection for the solar-wind hybrid renewable energy systems in Bangladesh using an integrated GIS-based BWM-fuzzy logic method. *Energy Convers. Manag.* **2023**, *283*, 116899. [CrossRef]

14. Gao, J.; Wang, Y.; Huang, N.; Wei, L.; Zhang, Z. Optimal site selection study of wind-photovoltaic-shared energy storage power stations based on GIS and multi-criteria decision making: A two-stage framework. *Renew Energy* **2022**, *201*, 1139–1162. [CrossRef]
15. Cheng, W.; Li, D.; Liu, Z.; Brown, R.D. Approaches for identifying heat-vulnerable populations and locations: A systematic review. *Sci. Total Environ.* **2021**, *799*, 149417. [CrossRef]
16. Abdelwahab, R.A.; Fekry, A.A.; Hamed, R.E.-D. The effective landscape design parameters with high reflective hardscapes: Guidelines for optimizing human thermal comfort in outdoor spaces by design -a case on hot arid climate weather. *Comput. Urban Sci.* **2025**, *5*, 28. [CrossRef]
17. Li, Y. Resilient Urban Design Concept in the Context of Climate Change. *Adv. Econ. Manag. Political Sci.* **2024**, *123*, 79–85. [CrossRef]
18. Pradhananga, A.K.; Davenport, M.A. Community attachment, beliefs and residents' civic engagement in stormwater management. *Landsc. Urban Plan.* **2017**, *168*, 1–8. [CrossRef]
19. Deilami, K.; Kamruzzaman, M.; Liu, Y. Urban heat island effect: A systematic review of spatio-temporal factors, data, methods, and mitigation measures. *Int. J. Appl. Earth Obs. Geoinf.* **2018**, *67*, 30–42. [CrossRef]
20. Derix, C. Digital masterplanning: Computing urban design. *Proc. Inst. Civ. Eng. Urban Des. Plan.* **2012**, *165*, 203–217. [CrossRef]
21. Arya, S. Harnessing Big Data and Machine Learning for Climate Change Predictions and Mitigation. In *Maintaining a Sustainable World in the Nexus of Environmental Science and AI.*; IGI Global: New York, NY, USA, 2024; pp. 383–408. [CrossRef]
22. Glover, F.; Glover, R.; Klingman, D. Computational study of an improved shortest path algorithm. *Networks* **1984**, *14*, 25–36. [CrossRef]
23. van Veghel, J.; Dane, G.; Agugiaro, G.; Borgers, A. Human-centric computational urban design: Optimizing high-density urban areas to enhance human subjective well-being. *Comput. Urban Sci.* **2024**, *4*, 13. [CrossRef]
24. Hanzl, M.; Tofiluk, A.; Zinowiec-Cieplik, K.; Grochulska-Salak, M.; Nowak, A. The Role of Vegetation in Climate Adaptability: Case Studies of Lodz and Warsaw. *Urban Plan* **2021**, *6*, 9–24. [CrossRef]
25. Carter, N. Greening the mainstream: Party politics and the environment. *Environ. Politics* **2013**, *22*, 73–94. [CrossRef]
26. Zhang, Y.; Luo, F. How are green spaces associated with chronic disease incidence in Australia? Direct health benefits and interactive effects with socioeconomic status based on multiple green space indicators. *Sustain. Cities Soc.* **2025**, *121*, 106229. [CrossRef]
27. Lenzholzer, S.; Carsjens, G.J.; Brown, R.D.; Tavares, S.; Vanos, J.K.; Kim, Y.; Lee, K. Awareness of urban climate adaptation strategies—An international overview. *Urban Climb* **2020**, *34*, 100705. [CrossRef]
28. Fahmy, M.; Ibrahim, Y.; Hanafi, E.; Barakat, M. Would LEED-UHI greenery and high albedo strategies mitigate climate change at neighborhood scale in Cairo, Egypt? *Build. Simul.* **2018**, *11*, 1273–1288. [CrossRef]
29. Alharthi, M.A.; Lenzholzer, S.; Cortesão, J. Climate responsive design in urban open spaces in hot arid climates: A systematic literature review. *Discov. Cities* **2025**, *2*, 38. [CrossRef]
30. El Dallal, N.; Visser, F. A climate responsive urban design tool: A platform to improve energy efficiency in a dry hot climate. *Int. J. Sustain. Energy* **2017**, *36*, 738–753. [CrossRef]
31. Yang, F.; Chen, L. *High-Rise Urban Form and Microclimate*; Springer: Singapore, 2020. [CrossRef]
32. Wong, C.H.H.; Cai, M.; Ren, C.; Huang, Y.; Liao, C.; Yin, S. Modelling building energy use at urban scale: A review on their account for the urban environment. *Build. Environ.* **2021**, *205*, 108235. [CrossRef]
33. Yang, Y.; Gatto, E.; Gao, Z.; Buccolieri, R.; Morakinyo, T.E.; Lan, H. The "plant evaluation model" for the assessment of the impact of vegetation on outdoor microclimate in the urban environment. *Build. Environ.* **2019**, *159*, 106151. [CrossRef]
34. Naser, M.Z.; Chehab, A.I. Materials and design concepts for space-resilient structures. *Prog. Aerosp. Sci.* **2018**, *98*, 74–90. [CrossRef]
35. Norton, B.A.; Coutts, A.M.; Livesley, S.J.; Harris, R.J.; Hunter, A.M.; Williams, N.S.G. Planning for cooler cities: A framework to prioritise green infrastructure to mitigate high temperatures in urban landscapes. *Landsc. Urban Plan.* **2015**, *134*, 127–138. [CrossRef]
36. Abdelmejeed, A.Y.; Gruehn, D. Optimizing an efficient urban tree strategy to improve microclimate conditions while considering water scarcity: A case study of Cairo. *Discov. Sustain.* **2024**, *5*, 66. [CrossRef]
37. Mokhtar, H.; Fahmy, M.; Gira, A. Climate Based Design Decision Support for Urban Village Development: A case study in Nuba, Egypt. *Int. Conf. Civ. Archit. Eng.* **2012**, *9*, 1–15. [CrossRef]
38. Wang, Y.; Zacharias, J. Landscape modification for ambient environmental improvement in central business districts—A case from Beijing. *Urban For. Urban Green.* **2015**, *14*, 8–18. [CrossRef]
39. Mukkavaara, J.; Shadram, F. An integrated optimization and sensitivity analysis approach to support the life cycle energy trade-off in building design. *EnergyBuild* **2021**, *253*, 111529. [CrossRef]
40. Cugurullo, F.; Caprotti, F.; Cook, M.; Karvonen, A.; McGuirk, P.; Marvin, S. The rise of AI urbanism in post-smart cities: A critical commentary on urban artificial intelligence. *Urban Stud.* **2024**, *61*, 1168–1182. [CrossRef]

41. Marvin, S.; While, A.; Chen, B.; Kovacic, M. Urban AI in China: Social control or hyper-capitalist development in the post-smart city? *Front. Sustain. Cities* **2022**, *4*, 1030318. [CrossRef]
42. Golubchikov, O.; Thornbush, M. Artificial Intelligence and Robotics in Smart City Strategies and Planned Smart Development. *Smart Cities* **2020**, *3*, 1133–1144. [CrossRef]
43. Ryan, Y.; Gutman, G. Aging, artificial intelligence, and the built environment in smart cities: Ethical considerations. *Gerontechnology* **2023**, *22*, 1–5. [CrossRef]
44. Luusua, A.; Ylipulli, J.; Foth, M.; Aurigi, A. Urban AI: Understanding the emerging role of artificial intelligence in smart cities. *AI Soc* **2023**, *38*, 1039–1044. [CrossRef] [PubMed]
45. Farooq, S.; Farooq, B.; Basheer, S.; Walia, S. *Balancing Environmental Sustainability and Privacy Ethical Dilemmas in AI-Enabled Smart Cities*; IGI Global Scientific Publishing: Hershey, PA, USA, 2023; pp. 263–286. [CrossRef]
46. Cong, C.; Page, J.; Kwak, Y.; Deal, B.; Kalantari, Z. AI Analytics for Carbon-Neutral City Planning: A Systematic Review of Applications. *Urban Sci.* **2024**, *8*, 104. [CrossRef]
47. Liu, Y.; Qin, S.; Li, J.; Jin, T. Artificial Intelligence and Street Space Optimization in Green Cities: New Evidence from China. *Sustainability* **2023**, *15*, 16367. [CrossRef]
48. Dogan, T.; Yang, Y.; Samaranayake, S.; Saraf, N. Urbano: A Tool to Promote Active Mobility Modeling and Amenity Analysis in Urban Design. *Technol. | Archit. + Des.* **2020**, *4*, 92–105. [CrossRef]
49. Veisi, O.; Shakibamanesh, A.; Rahbar, M. Using intelligent multi-objective optimization and artificial neural networking to achieve maximum solar radiation with minimum volume in the archetype urban block. *Sustain. Cities Soc.* **2022**, *86*, 104101. [CrossRef]
50. Camporeale, P.E.; Mercader-Moyano, P. Towards nearly Zero Energy Buildings: Shape optimization of typical housing typologies in Ibero-American temperate climate cities from a holistic perspective. *Sol. Energy* **2019**, *193*, 738–765. [CrossRef]
51. Xu, X.; Liu, Y.; Wang, W.; Xu, N.; Liu, K.; Yu, G. Urban layout optimization based on genetic algorithm for microclimate performance in the cold region of China. *Appl. Sci.* **2019**, *9*, 747. [CrossRef]
52. Wortmann, T.; Cichocka, J.; Waibel, C. Simulation-based optimization in architecture and building engineering—Results from an international user survey in practice and research. *EnergyBuild* **2022**, *259*, 111863. [CrossRef]
53. Badii, C.; Bellini, P.; Cenni, D.; Chiordi, S.; Mitolo, N.; Nesi, P.; Paolucci, M. Computing 15MinCityIndexes on the Basis of Open Data and Services. In Proceedings of the Computational Science and Its Applications—ICCSA 2021, Cagliari, Italy, 13–16 September 2021; pp. 565–579. [CrossRef]
54. Xiaofang, S.; Ying, X.; Ning, G.; Jingru, Y. A Computation Model for Proximity. In Proceedings of the 2024 IEEE 2nd International Conference on Image Processing and Computer Applications (ICIPCA), Shenyang, China, 28–30 June 2024; IEEE: Piscataway, NJ, USA, 2024; pp. 75–78. [CrossRef]
55. Pretzsch, H.; Biber, P.; Uhl, E.; Dahlhausen, J.; Rötzer, T.; Caldentey, J.; Koike, T.; van Con, T.; Chavanne, A.; Seifert, T.; et al. Crown size and growing space requirement of common tree species in urban centres, parks, and forests. *Urban Urban Green* **2015**, *14*, 466–479. [CrossRef]
56. Bayer, D.; Seifert, S.; Pretzsch, H. Structural crown properties of Norway spruce (*Picea abies* [L.] Karst.) and European beech (*Fagus sylvatica* [L.]) in mixed versus pure stands revealed by terrestrial laser scanning. *Trees—Struct. Funct.* **2013**, *27*, 1035–1047. [CrossRef]
57. Heldens, W.; Taubenböck, H.; Esch, T.; Heiden, U.; Wurm, M. Analysis of surface thermal patterns in relation to urban structure types: A case study for the city of Munich. *Remote Sens. Digit. Image Process.* **2013**, *17*, 475–493. [CrossRef]
58. Enquist, B.J.; West, G.B.; Brown, J.H. Extensions and evaluations of a general quantitative theory of forest structure and dynamics. *Proc. Natl. Acad. Sci. USA* **2009**, *106*, 7046–7051. [CrossRef] [PubMed]
59. Ishii, H.T.; Tanabe, S.I.; Hiura, T. Exploring the relationships among canopy structure, stand productivity, and biodiversity of temperate forest ecosystems. *For. Sci.* **2004**, *50*, 342–355. [CrossRef]
60. Jim, C.Y. Resolving intractable soil constraints in urban forestry through research–practice synergy. *Socioecon. Pract. Res.* **2019**, *1*, 41–53. [CrossRef]
61. Lai, A.; Maing, M.; Ng, E. Observational studies of mean radiant temperature across different outdoor spaces under shaded conditions in densely built environment. *Build. Environ.* **2017**, *114*, 397–409. [CrossRef]
62. Abdelmejeed, A.Y.; Gruehn, D. Optimization of Microclimate Conditions Considering Urban Morphology and Trees Using ENVI-Met: A Case Study of Cairo City. *Land* **2023**, *12*, 2145. [CrossRef]
63. Meliouh, F.; Ghanemi, F.; Hamel, K.; Nasri, M.; Makhloufi, S. Greening the arid: The impact of urban vegetation on the outdoor thermal comfort in hot and dry city. *South Fla. J. Dev.* **2024**, *5*, e4718. [CrossRef]
64. Yin, Y.; Li, S.; Xing, X.; Zhou, X.; Kang, Y.; Hu, Q.; Li, Y. Cooling Benefits of Urban Tree Canopy: A Systematic Review. *Sustainability* **2024**, *16*, 4955. [CrossRef]
65. Naboni, E.; Natanian, J.; Brizzi, G.; Florio, P.; Chokhachian, A.; Galanos, T.; Rastogi, P. A digital workflow to quantify regenerative urban design in the context of a changing climate. *Renew. Sustain. Energy Rev.* **2019**, *113*, 109255. [CrossRef]

66. Kirste, K.K.; Monge, P.R. Computing dynamic organizational proximity: The PROXTIME computer program. *Behav. Res. Methods Instrum.* **1983**, *15*, 89–90. [CrossRef]
67. Lima, F.T.; Costa, F. The Quest for Proximity: A Systematic Review of Computational Approaches towards 15-Minute Cities. *Architecture* **2023**, *3*, 393–409. [CrossRef]

Disclaimer/Publisher's Note: The statements, opinions and data contained in all publications are solely those of the individual author(s) and contributor(s) and not of MDPI and/or the editor(s). MDPI and/or the editor(s) disclaim responsibility for any injury to people or property resulting from any ideas, methods, instructions or products referred to in the content.